# A+ Indexes: Lightweight and Highly Flexible Adjacency Lists for Graph Database Management Systems

Amine Mhedhbi, Pranjal Gupta, Shahid Khaliq, Semih Salihoglu
University of Waterloo
{amine.mhedhbi, pranjal.gupta, shahid.khaliq, semih.salihoglu}@uwaterloo.ca



## ABSTRACT

Graph database management systems (GDBMSs) are highly optimized to perform very fast joins of vertices by indexing the neighbourhoods of vertices in adjacency list indexes. However, existing GDBMSs have system-specific and fixed adjacency list index structures, which makes each system highly efficient on only a fixed set of workloads. We describe a highly flexible and lightweight indexing sub-system for GDBMSs, that is coupled with materialized view capability, that we call *A+ indexes*. A+ indexes comprise of three components. *Default A+ indexes* provide flexibility to users to index neighbourhoods of vertices using arbitrary nested secondary partitioning and sorting criteria. This allows users to optimize a system for a variety of workloads with no or minimal memory overheads. *Secondary vertex- and edge-bound A+ indexes*, respectively are views over edges and 2-paths. Edge-bound indexes partition views over 2-paths by edge IDs and store the neighbourhoods of edges instead of vertices. Our secondary indexes are designed to have a very lightweight implementation based on a technique we call *offset lists*. A+ indexes allow a wider range of applications to benefit from GDBMSs' fast join capabilities. We demonstrate the flexibility, efficiency, and low memory overheads of A+ indexes through extensive experiments on a variety of applications.

## 1. INTRODUCTION

The term *graph database management system* (GDBMS) in its contemporary usage refers to data management software such as Neo4j [33], JanusGraph [24], TigerGraph [46], and GraphflowDB [25, 32] that adopt the property graph data model [34]. In this model, application data is represented as a set of vertices, which represent the entities in the application, directed edges, which represent the connections between entities, and arbitrary key value properties on the vertices and edges. GDBMSs have lately gained popularity among a wide range of applications from fraud detection and risk assessment in financial services to recommendations in e-commerce and social networks [41].

One reason GDBMSs appeal to users is that they are highly optimized to perform very fast joins of vertices. While systems use traditional B+ trees to access vertices with certain properties in scan operations, join operators access neighbourhoods of vertices through *adjacency list indexes* [11]. Adjacency list indexes are constant-depth data structures that partition the edge records into lists by source or destination vertex IDs, and sometimes also by an additional criteria, e.g., the labels of the edges and provide very fast access to neighbourhoods of vertices. Some systems further sort these lists according to some properties. This contrasts with tree-based indexes, such as B+ trees, which have logarithmic depth in the size of the data they index. Although GDBMSs give flexibility to their users to index vertices in different B+ trees, they do not provide any flexibility in indexing the neighbourhoods of vertices. Specifically, GDBMSs make different but fixed choices about the partitioning and sorting criteria of their adjacency list indexes, making each system highly efficient on only a fixed set of workloads. This creates physical data dependence, as users have to model their data, e.g., pick their edge labels, according to the fixed partitioning and sorting criteria of their systems.

We address the following question: *How can the fast join capabilities of GDBMSs be expanded to a much wider set of workloads?* We describe a highly flexible and lightweight adjacency list indexing sub-system for GDBMSs, that is coupled with materialized view capability, that we call *A+ indexes*. We observe that lists in existing adjacency list indexes are effectively *local views* over the edges that have fast access paths and are used by systems to evaluate queries. We first give users flexibility in selecting the partitioning and sorting criteria of the system's *default A+ indexes*, which provides access to a wider set of local views over the edges. Then, we support defining two types of *global views*: (i) views over edges that satisfy arbitrary predicates that are stored in *secondary vertex-bound A+ indexes*; (ii) views over 2-paths that are stored in *secondary edge-bound A+ indexes*, which extends the notion of neighbourhood from vertices to edges. We describe a very lightweight implementation of our secondary indexes through a technique we call *offset lists*, which take often one or two bytes per indexed edge.

We next review the adjacency list indexes of existing systems and then give an overview of A+ indexes. Figure 1 shows an example financial graph that we use as a running example. The graph contains vertices with `Customer` and `Account` labels. `Customer` vertices have `name` properties and `Account` vertices have `city` and `accountType(acc)` properties. From customers to accounts are edges with `Owns(O)` labels and between accounts are transfer edges with `Dir-Deposit(DD)` and `Wire(W)` labels with `amount(amt)`, `currency`, and `date` properties. We omit dates in the figure and give each transfer edge an ID such that $t_i.date < t_j.date$ if $i < j$.

### 1.1 Overview of Existing Adjacency Lists

Adjacency lists are accessed by a GDBMS's operators that join

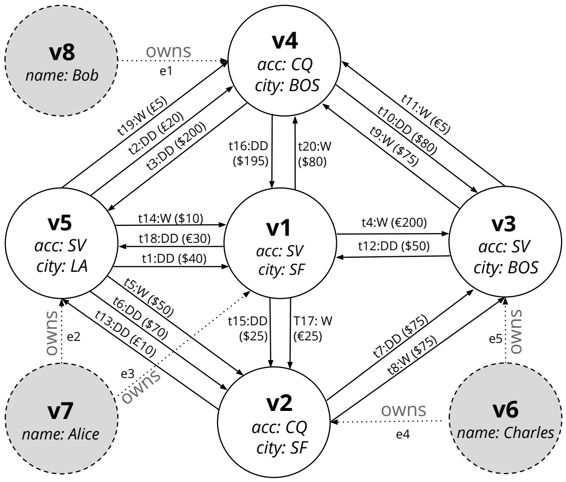


Figure 1: Example financial graph.

vertices, e.g., the EXPAND operator in Neo4j or EXTEND/INTERSECT in GraphflowDB. GDBMSs employ two broad techniques to provide fast access to adjacency lists while performing these joins: **(1) Partitioning:** Every GDBMS partitions its edges first by their source or destination vertex IDs, respectively in *forward* and *backward* indexes. We call this the primary partitioning criteria.

EXAMPLE 1. *Consider the following query, written in openCypher [38], that finds 2-paths starting from a vertex with name "Alice". Below, $a_i$ and $r_j$ are variables for, respectively, the query vertices and query edges.*

MATCH $a_1{-}[r_1]{-}{>}a_2{-}[r_2]{-}{>}a_3$
WHERE $a_1.name$ = '*Alice*'

*In every GDBMS we know of, this query is evaluated in three steps: (1) scan the vertices and find a vertex with* `name` *"Alice" and match $a_1$. In our example graph,* `v7` *would match $a_1$; (2) access* `v7`*'s forward adjacency list, often with one lookup, to match $a_1 \rightarrow a_2$ edges; and (3) access the forward lists of matched $a_2$'s to match $a_1 \rightarrow a_2 \rightarrow a_3$ paths.*

Some GDBMSs employ secondary partitioning on these lists, e.g., Neo4j [33] further partitions each vertex's list by edge labels. This allows accessing more granular lists in constant or close to constant time without running any predicates.

EXAMPLE 2. *Consider the following query that returns all* `Wire` *transfers made from the accounts Alice* `Owns`*:*

MATCH $a_1{-}[r_1{:}O]{-}{>}a_2{-}[r_2{:}W]{-}{>}a_3$
WHERE $a_1.name$ = '*Alice*'

*The "$r_1$:*`O`*" is syntactic sugar in Cypher for the* `r1.label= Owns` *predicate. A system with lists partitioned by vertex IDs and edge labels can evaluate this query as follows. First, find* `v7`*, with name "Alice", and then access* `v7`*'s* `Owns` *edges, often with a constant number of lookups and without running any predicates, and match $a_2$'s. Finally access the* `Wire` *edges of each $a_2$ to match the $a_3$'s.*

**(2) Final List Sorting:** Some systems further sort their most granular lists according to an edge property [24] or the IDs of the neighbours in the lists [4, 32]. Sorting enables systems to access parts of lists in time logarithmic in the size of lists.

Similar to major and minor sorts in traditional indexes, partitioning and sorting keeps the edges in a sorted order, allowing systems to use fast intersection-based join algorithms, such as worst-case optimal (WCO) joins [36, 37] or sort-merge joins.

| A+ Index | Global View | Pr. Part. | Stored Lists |
|---|---|---|---|
| Default | `Edge` | vertex ID | ID Lists |
| Secondary VB | $\sigma$`Edge` | vertex ID | Offset Lists |
| Secondary EB | $\sigma$`Edges`$\bowtie$`Edges` | edge ID | Offset Lists |

Table 1: Three types of A+ indexes. VB, EB, and Pr. Part. stand for vertex-bound, edge-bound, and primary partitioning, respectively. All indexes allow nested secondary partitioning on categorical properties of the indexed adjacent edges and neighbours. The partitioning criteria determines the final local views that each list stored in an index corresponds to. In addition all indexes allow sorting on the indexed adjacent edges and neighbours properties.

EXAMPLE 3. *Consider the following query that finds all cyclical wire transfers with 3 edges involving Alice's account $v1$.*

MATCH $a_1{-}[r_1{:}W]{-}{>}a_2{-}[r_2{:}W]{-}{>}a_3,\ a_3{-}[r_3{:}W]{-}{>}a_1$
WHERE $a_1$.ID=$v1$

*In systems that implement WCO joins, such as EmptyHeaded [4] or GraphflowDB [32], this query is evaluated by scanning each* `v1`$\rightarrow a_2$ `Wire` *edge and intersecting the pre-sorted* `Wire` *lists of* `v1` *and $a_2$ to match the $a_3$ vertices.*

To provide very fast access to each list, lists are accessed through data structures that have constant depth, instead of logarithmic depths of traditional tree-based indexes. This is achieved by having one level in the index for each partitioning criteria, so levels in the index are not constrained to have a fixed order, e.g., k as in a k-ary tree. This makes GDBMSs very fast when accessing the appropriate neighbourhoods of vertices as they perform certain joins. However, existing GDBMSs adopt fixed system-specific partitioning and possibly sorting criteria, which has two main shortcomings: (1) users need to model their data, e.g. pick vertex and edge labels, considering the system's physical design decisions, creating physical data dependence; and (2) systems can provide fast joins for only the workloads that have equality predicates on the system-specific properties that are used as partitioning and sorting criteria.

## 1.2 Overview of A+ Indexes

Table 1 summarizes the high-level properties of the three components of A+ indexes, which we next review.
**Default A+ Indexes:** Instead of a system-specific fixed criteria, users can provide arbitrary nested partitioning and sorting on the system's default indexes. The edges are then indexed in a nested compressed sparse-row-like data structure that has as many levels as there are partitioning criteria. The most granular lists are then sorted according to the given sorting criteria. Figure 2a shows an example default A+ index on our running example that has two nested partitioning levels on top of the primary vertex ID partitioning: (i) by edge labels; and (ii) by `currency` property. This allows the system to provide fast joins for workloads that access edges that satisfy other equality predicates without data remodelling and with no or negligible memory costs, leading to significant performance gains in some settings.
**Secondary A+ Indexes:** We observe that each level of existing indexes identifies a sub-list, which is effectively a view over edges that is limited to satisfying a different set of equality predicates (determined by the partitioning criteria). Figure 2a shows the nested sub-lists with different types of boxes. For example, the red dashed box corresponds to view $\sigma_{\text{srcID=v1}}$`E`, while the blue dash-dotted box corresponds to $\sigma_{\text{srcID=v1 \& e.label=Owns}}$`E`, where `E` is the set of all edges. Therefore query processors of existing systems effectively evaluate queries using views when they probe adjacency lists to access these lists. We refer to views that sub-lists correspond to as *local views*.

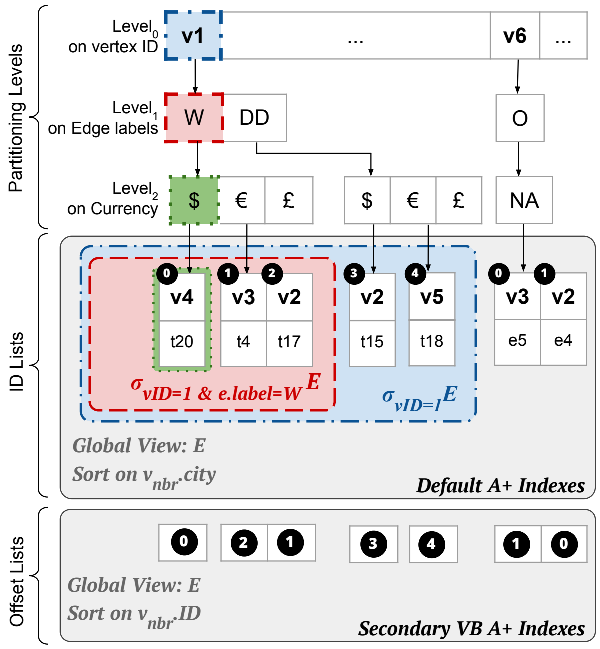


(a) Example default A+ Index and a secondary vertex-bound A+ Index.

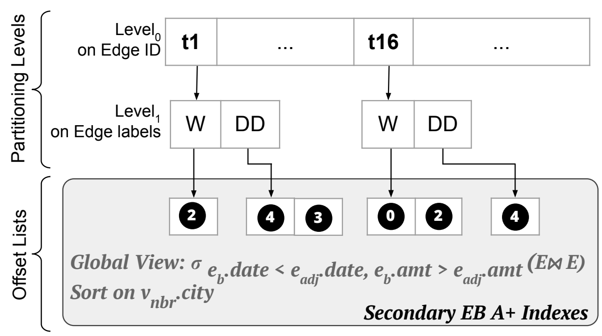


(b) Example secondary edge-bound A+ Index.

Figure 2: Example A+ indexes on our running example.

One can also think of the entire adjacency list index as one *global view*, which in Figure 2a is simply the set of edges, shown in a solid grey box. To support access to a larger set of views, we first allow users to define two other types of global views that are indexed in our *secondary A+ indexes*. Our choice of the views we support allows us to provide a lightweight implementation with an appropriate partitioning, which we discuss momentarily.

(i) Global views on the edges that satisfy arbitrary predicates, such as transfers with `amount`>1000 USD or made to accounts with `balance` > 5000. These are stored in *secondary vertex-bound A+ indexes* and partitioned primarily by vertex IDs.
(ii) Global views over 2-paths, which are stored in *secondary edge-bound A+ indexes* and partitioned primarily by edge IDs.

Edge-bound indexes extend the notion of adjacency from vertices to edges, which is highly beneficial for some applications.

EXAMPLE 4. *Consider the following query, which is the core of an important class of queries in financial fraud detection*[1].

[1]Communication with developers of GaussDB [18], a DBMS supporting a graph data model and used by multiple financial institutions in production.

MATCH $a_1$–$[r_1{:}]$–>$a_2$–$[r_2{:}]$–>$a_3$–$[r_3{:}]$–>$a_4$
WHERE $r_1$.eID=$t13$,
$r_1.amt{>}r_2.amt,\ r_1.amt{<}r_2.amt\ +\alpha,\ r_1.date{<}r_2.date,$
$r_2.amt{>}r_3.amt,\ r_2.amt{<}r_3.amt\ +\alpha,\ r_2.date{<}r_3.date$

*The query searches a three-step money flow path from a transfer edge with* `eID t13` *where each additional transfer (*`Wire` *or* `Dir-Deposit`*) happens at a later date and for a smaller amount of at most α, simulating some money flowing through the network with intermediate hops taking cuts.*

The predicates of this query compare properties of an edge on a path with the previous edge on the same path. A system matches $r_1$ to `t13`, which is from vertex `v2` to `v5`. Existing systems have to read transfer edges from `v5` and filter those that have a later `date` value than `t13` and also have the appropriate `amount` value. Instead, when the next query edge to match $r_2$ has predicates depending on the query edge $r_1$, these queries can be evaluated much faster if adjacency lists are partitioned by edge IDs: a system can directly access the *forward adjacency list of* `t13`, i.e., edges whose `srcID` are `v5`, that satisfy the predicate on the `amount` and `date` properties that depend on `t13`, and perform the extension. Our edge-bound indexes allow the system to generate plans that perform this much faster processing.

**Lightweight Offset Lists:** Storing secondary A+ indexes requires data duplication and consumes extra memory. Our approach to addressing the memory footprint of secondary indexes is based on two important observations: (1) each list in every secondary index is a subset of some list in the default index, which is a result of our design of secondary indexes; and (2) each list in default indexes contains a very small number of edges, which is a result of the sparsity, i.e., small average degrees, of real-world graphs. Therefore, instead of duplicating the globally identifiable edge and neighbour IDs that need to be stored in the *ID lists* of default indexes, secondary indexes can be stored with much smaller, often one or two byte, list-level identifiable pointers into systems' default lists. We refer to these lists as *offset lists*. Figures 2a and 2b show example offset lists, respectively, for a secondary vertex-bound and edge-bound A+ indexes. When join operators read actual edges through offset lists, access is made to non-consecutive but very close memory locations, achieving high CPU cache locality. We demonstrate that secondary vertex-bound and edge-bound indexes can have very small memory overheads, as low as a few percentage points, making them highly practical.

## 2. A+ INDEXES

This section describes our indexing sub-system. There are three types of indexes in our indexing sub-system: (i) default A+ indexes; (ii) secondary vertex-bound A+ indexes; and (iii) secondary edge-bound A+ indexes. Each index, both in our solution and existing systems, stores a set of adjacency lists, each of which stores a set of edges. We refer to the edges that are stored in the lists as *adjacent* edges, and the vertices that adjacent edges point to as *neighbour* vertices. So in vertex ID partitioned lists, neighbours refer to destination vertices in forward indexes and source vertices in backward indexes. We next give an overview of each index. We cover the lightweight implementation of secondary A+ indexes in Section 3.

### 2.1 Default A+ Indexes

Default A+ indexes are the primary and by default the only indexes in our indexing sub-system. These indexes are required to contain each edge in the graph, otherwise the system will not be able to answer some queries. Similar to the adjacency lists of existing systems, there are two default indexes, one forward and one backward, partitioned primarily by the source and destination vertex IDs of the edges, respectively. In our implementation in GraphflowDB, by default we adopt secondary partitioning by edge labels and sorting according to the IDs of the neighbours, which optimizes the system for queries with edge labels and matching cyclic subgraphs using intersection-based join plans. However, unlike existing systems, users can reconfigure the secondary partitioning and sorting criteria of the systems' default. This reconfiguration has no or very minor memory costs and can make the system significantly fast on a variety of workloads. As we explain in Sections 2.2.1 and 2.2.2 momentarily, the default indexes are also the reference indexes to which secondary indexes point.

### 2.1.1 Flexible Secondary Partitioning

Default A+ indexes can contain nested secondary partitioning criteria on any categorical property of adjacent edges as well as neighbour vertices, such as edge or neighbour vertex labels, or the `currency` property on the edges in our running example. In our implementation we allow integers or enums that are mapped to small number of integers as categorical values. Because graph data is not structured, not all edges need to contain the properties on which the secondary partitionings happen. Edges with null property values form a special partition.

Each provided secondary partitioning adds one new layer to the index, storing offsets to a particular slice of the next layer, where the last level contains the final list containing the neighbourhood of one vertex (because the primary partitioning is by vertex ID). We refer to the final lists in the default indexes as *ID lists*, as they store the IDs of the edges and neighbour vertices. This is effectively a nested compressed sparse row-like compact physical storage that ensures that the full neighbourhood of each vertex is stored consecutively in memory.

EXAMPLE 5. *Consider querying all wire transfers made in USD currency from Alice's account and the destination accounts of these transfers:*

MATCH $a_1\!-\![r_1{:}O]\!-\!>a_2\!-\![r_2{:}W]\!-\!>a_3$
WHERE $a_1.name$ = '$Alice$', $r_2.currency{=}USD$

*Here the query plans of existing systems that partition by edge labels will read all `Wire` edges from Alice's account and, for each edge, read its `currency` property and run a predicate to verify whether or not it is in USD.*

Instead, if queries with equality predicates on the `currency` property are important and frequent for an application, users can reconfigure their default A+ indexes to provide a secondary partitioning based on `currency`.

RECONFIGURE DEFAULT INDEX
PARTITON BY $e_{adj}.label,\ e_{adj}.currency$
SORT BY $v_{nbr}.city$

In index creation and modification commands, we use reserved keywords $e_{adj}$ and $v_{nbr}$ to refer to adjacent edges and neighbours, respectively. The above command will reconfigure the adjacency lists to have two levels of secondary partitioning, first by the edge labels and then by the currency property of these edges, which will point to sub-lists that are sorted by the `city` property of the neighbour vertices (discussed momentarily). Figure 2a shows the final physical design this generates as an example on our running example. For the query in Example 5, the system's join operator can now directly access these more granularly partitioned lists, first by wire and the by USD, as it accesses Alice's neighbourhood, without running any predicates.

Note that each level of the index can be used to access a different sub-list in the final lists to access a set of edges that satisfy different properties. For example the more granularly partitioned lists in Figure 2a still allow access to only the `Wire` edges of a vertex, because the part of the ID list that contains wire edges are still contiguous and their offsets can be found by inspecting the offsets in the first and second levels of the index.

### 2.1.2 Flexible ID List Sorting

The most granular sub-lists can be sorted according to one or more arbitrary properties of the adjacent edges or neighbour vertices, e.g., the `date` property of `Transfer` edges and the `city` property of the `Account` vertices of our running example. Similar to partitioning, edges with null property values on which the sorting is are ordered last. Secondary partitioning and sorting criteria together store the neighbourhoods of vertices in a particular sort order, allowing a system to generate intersection-based join plans for a wider set of queries.

EXAMPLE 6. *Consider the following query that searches for a three-branched money transfer tree, consisting of wire and direct deposit transfers, emanating from an account with `vID v5` and ending in three sink accounts in the same city.*

MATCH $a_1\!-\![{:}W]\!-\!>a_2\!-\![{:}W]\!-\!>a_3,$
$a_1\!-\![{:}W]\!-\!>a_4$
$a_1\!-\![{:}DD]\!-\!>a_5\!-\![{:}DD]\!-\!>a_6$
WHERE $a_1.\mathrm{ID}{=}v5,\ a_3.city{=}a_4.city{=}a_6.city$

*If `Wire` and `Dir-Deposit` lists are partitioned or sorted by `city`, as in in Figure 2a, after matching $a_1{\rightarrow}a_2$ and $a_1{\rightarrow}a_5$, a plan can directly intersect two `Wire` lists of $a_1$ and $a_2$ and one `Dir-Deposit` list of $a_5$ in a single operation to find the flows that end up in accounts in the same city. Such plans are not possible with the adjacency list indexes of existing systems.*

Observe that the ability to reconfigure the system's default A+ indexes provides more physical data independence. Users do not have to model their datasets according to the system's default physical design and changes in the workloads can be addressed simply with index reconfigurations. We will demonstrate the benefits of this flexibility and the minor memory overheads of default index reconfigurations in our evaluations.

## 2.2 Secondary A+ Indexes

Many indexes in DBMSs can be thought as data structures that give fast access to *views*. In our context, each sub-list in the default indexes is effectively a *local view* over edges. For example, the dashed red in Figure 2a is the $\sigma_{\text{srcID=v1 \&e.label=Wire}}$`Edge` local view while the dotted green box encloses a more granular local view corresponding to $\sigma_{\text{srcID=1 \& e.label=wire \& curr=USD}}$`Edge`. One can also think of the entire index as indexing a *global view*, which for default indexes is simply the `Edge` table. Therefore the local views that can be obtained through the system's default A+ indexes are constrained to views over the edges that contain an equality predicate on the source or destination ID (due to vertex ID partitioning) and one equality predicate for each secondary partitioning criteria. To provide access to even wider set of local views, a system should support more general materialized views and index these in adjacency list indexes. We next describe two types of secondary A+ indexes, which are coupled with two types of global views and two different ways of partitioning these views. These specific global views and their partitioning allows us to provide a lightweight implementation, which we describe in Section 3.

(i) *Secondary vertex-bound A+ indexes* index global views over edges with arbitrary predicates. These views are primarily partitioned by vertex IDs.

(ii) *Secondary edge-bound A+ indexes* index global views over 2-paths. These views are partitioned by edge IDs and effectively store neighbourhoods of edges.

In the rest, when a particular adjacency list is bound to a vertex, say $v1$, or an edge, we refer to that vertex or edge as the *bound vertex* and *bound edge*, respectively.

### 2.2.1 Secondary Vertex-Bound A+ Indexes

Secondary vertex-bound indexes index global views over edges that contain arbitrary selection predicates. These views cannot contain other operators, such as group by's, aggregations, or projections, so their outputs are a subset of the original edges. The predicates used in these global views can depend on the bound vertex, adjacent edge, or neighbour vertex. Secondary vertex-bound A+ indexes store these global views with a primary partitioning on vertex IDs and the same partitioning and sorting flexibility provided in default A+ indexes. In order to use secondary vertex-bound A+ indexes, users need to first define the global view over the edges and then define the structure of the secondary vertex-bound A+ index.

EXAMPLE 7. *Consider a fraud detection application that searches money flow patterns with high amount of transfers, say over 10000 USDs. We can create a secondary vertex-bound index to index those edges in lists, partitioned first by vertices and then possibly by other properties and in a sorted manner as before.*

CREATE EDGE VIEW LargeUSDTrnx
MATCH $v_s{-}[e_{adj}]{-}{>}v_d$
WHERE $e_{adj}.currency{=}USD,\ e_{adj}.amt{>}10000$
INDEX AS FW–BW
PARTITION BY $e_{adj}.label$
SORT BY $v_{nbr}.ID$

Above, $v_s$ and $v_d$ are keywords to refer to the source and destination vertices, whose properties can be accessed in the WHERE clause. FW and BW are keywords to build the index in the forward or backward direction, a partitioning option given to users. FW-BW indicates double indexing the edges both in the forward and backward directions. The most granular sub-lists of the resulting secondary vertex-bound A+index effectively materializes a local view of the form $\sigma_{\text{srcID=* \& elabel=* \& curr=USD \& amount > 10000}}$`Edge`. If such views or views that correspond to other levels of the index appear as part of the subgraph patterns, systems can directly access these views and avoid evaluating the predicates in these views.

### 2.2.2 Edge-Bound A+ Indexes

Vertex-bound adjacency lists store the edges that are immediately in the neighbourhood of each vertex. Our edge-bound indexes extend the notion to define neighbourhoods of edges. This can benefit applications in which the searched patterns concern relations between two adjacent, i.e., consecutive, edges, as in the money flow patterns from Example 4. Specifically, secondary edge-bound indexes index global views over 2-path. As before, these views cannot contain other operators, such as group by's, aggregations, or projections, so their outputs are a subset of 2-paths. The view has to specify a predicate and that predicate has to access properties of both edges in 2-paths. We explain this requirement momentarily. Secondary edge-bound indexes store these global views with a primary partitioning *on edge IDs* and, as before, the same partitioning and sorting flexibility provided in default A+ indexes. There are three possible 2-paths, $\rightarrow\rightarrow$, $\rightarrow\leftarrow$, and $\leftarrow\leftarrow$, when partitioned by different edges gives four unique possible ways in which an edge's neighbourhood can be defined.

(i) Destination-Forward: $v_s{-}[e_b]{\rightarrow}v_d{-}[e_{adj}]{\rightarrow}v_{nbr}$

(ii) Destination-Backward: $v_s{-}[e_b]{\rightarrow}v_d{\leftarrow}[e_{adj}]{-}v_{nbr}$

(iii) Source-Forward: $v_{nbr}{-}[e_{adj}]{\rightarrow}v_s{-}[e_b]{\rightarrow}v_d$

(iv) Source-Backward: $v_{nbr}{\leftarrow}[e_{adj}]{-}v_s{-}[e_b]{\rightarrow}v_d$

$e_b$ is the edge that the adjacency lists will be bound to, and $v_s$ and $v_d$ refer to the source and destination vertices of $e_b$, respectively. For example, we refer to the first 2-path view as destination-forward because partitioning those paths by $e_b$ stores the forward edges of the destination vertex of the bound edge.

EXAMPLE 8. *Consider creating an index for the sequence of adjacent edges in the money flow queries from Example 4.*

CREATE 2PATH VIEW MoneyFlow
MATCH $v_s{-}[e_b]{\rightarrow}v_d{-}[e_{adj}]{\rightarrow}v_{nbr}$
WHERE $e_b.date{<}e_{adj}.date,\ e_{adj}.amt{<}e_b.amt$
INDEX AS
PARTITION BY $e_{adj}.label$
SORT BY $v_{nbr}.city$

This query creates an edge-bound A+ index that, for each edge $t_i$, stores the forward edges from $t_i$'s destination vertex which were made at a later `date` and for a smaller `amount`, partitioned by the labels of the adjacent edges and sorted by the `city` property of the neighbouring vertices, i.e., the vertex that is not shared with $e_b$. Figure 2a shows the lists this index stores on our running example. The most granular sub-lists in the index correspond to views of the form: $\sigma_{e_b\text{.ID=* \& }e_{adj}\text{.label=* \& }e_b\text{.date < }e_{adj}\text{.date \& }e_b\text{.amt > }e_{adj}\text{.amt}}(\rho_{e_b}(E) \bowtie \rho_{e_{adj}}(E))$. `E` abbreviates `Edge` and the omitted join predicate is $e_b$.dstID=$e_{adj}$.srcID. Readers can verify that, in presence of this index, a GDBMS can evaluate the money flow query from Example 4, ignoring the predicate with $\alpha$, by scanning only one edge. It first scans `t13`'s and lists which contains a single edge `t19`. In contrast, even if all `Transfer` edges are directly accessible using a vertex-bound A+ index, a system would access 9 edges after scanning `t13`.

Observe that unlike vertex-bound A+ indexes, an edge $e$ in the graph can appear in multiple adjacency lists in an edge-bound index. For example, in Figure 2b, edge `t17` (having offset `2`) appear both in the adjacency list for `t1` as well as `t16`. As a consequence, we restrict that users have to specify a predicate in the WHERE clause that access properties of both edges in the 2-paths. We impose this restriction because if all the predicates are localized to a single query edge, say $v_s{-}[e_b]{\rightarrow}v_d$, then we would redundantly generate duplicate adjacency lists, and defining instead a secondary vertex-bound A+ index would give the same access path and avoid this redundancy. Consider as an example the following edge-bound A+ index:

CREATE 2PATH VIEW Redundant
MATCH $v_s{-}[e_b]{\rightarrow}v_d{-}[e_{adj}]{\rightarrow}v_{nbr}$
WHERE $e_{adj}.amt{<}10000$

In absence of an INDEX AS command, global views are only partitioned by the primary partitioning. Consider the account `v2` in our running example graph in Figure 1. For each of the four incoming edges of `v2`, namely `t5`, `t6`, and `t17`, this index would contain the same adjacency list that consists of all outgoing edges of `v2`: {`t7`,`t8`, `t13`, `t15`}, because the predicate is localized only to a single edge. Instead, a user can define a vertex-bound A+ index with the same predicate and bound it to `v2` and achieve the same access path to the edges {`t7`,`t8`,`t13`, `t15`}.

Views over edges and 2-paths that we support, with the specific edge ID partitioning of 2-paths have an important property that is conducive to a lightweight implementation, which we discuss next.

# 3. LIGHTWEIGHT OFFSET LISTS

The predominant memory cost of default indexes is the storage of the IDs of the adjacent edges and neighbour vertices in the *ID lists*. Because the IDs in these lists globally identify vertices and edges, their sizes need to be logarithmic in the number of edges and vertices in the graph, and often stored as 4 to 8 byte integers in systems. For example, in our implementation, edge IDs take 8 and neighbour IDs take 4 bytes.

In our indexing sub-system, default A+ index reconfiguration does not result in data duplication and its only memory overheads (or benefits) are from changes in the group values, which are minimal. In contrast, secondary indexes require extra memory and may have significant memory overheads. However, the lists in both secondary vertex-bound and edge-bound indexes have the important property that they are subsets of some list in the default adjacency lists: (i) a secondary vertex-bound list for $v_i$ is a subset of the list of $v_i$'s default ID list; (ii) an edge-bound list for $e_j = (v_s, v_d)$ is a subset of either $v_s$'s or $v_d$'s default ID list, depending on the direction of the index, e.g., $v_d$'s list for a `DST-FW` list. Recall that in our compressed-sparse-row-like implementation of the default indexes, the final lists of each vertex, i.e., the sub-lists after secondary partitionings, are contiguous. Therefore, instead of storing (edge ID, neighbour ID) pairs, we can store offsets to an appropriate ID list. We call these lists *offset lists*.

The average size of the lists is proportional to the average degree in the graph, which is often very small, in the order of tens or hundreds, in many real world graph data sets. This important property of real world graphs has two advantages:

1. Offsets need to be list-level identifiable and take a small number bytes. Specifically, in our implementation, offsets take less than two bytes on average. Naturally, the final memory consumptions of ID and offset lists depend on other optimizations system designers make, such as ID compression schemes. For example, on many of our graphs, the edge IDs can be compressed to 4 or 5 bytes instead of 8, and the offsets in offset lists can be compressed to a few bits instead of a few bytes. Importantly, irrespective of these optimizations, globally identifiable IDs require sizes logarithmic in the number of edges and vertices in the graph (tens or hundreds of millions), while list-level identifiable offsets require sizes logarithmic in the average list sizes (tens or hundreds in many real-world graphs).
2. Reading the original edge and neighbour IDs through offset lists require an indirection and lead to reading not-necessarily consecutive locations in memory. However, because the lists sizes are small, we still get a very good CPU cache locality. We will demonstrate this benefit momentarily.

We implement each secondary index in one of two possible ways, depending on whether the index contains any predicates and whether its secondary partitioning structure matches the secondary partitioning structure of the default A+ indexes.

- *With no predicates and same secondary partitioning*: The lists of the secondary index store the same lowest-level local views as the lists of the default index but in a different sort order. Therefore, we only store the offset lists of the index, which contain the same number of elements as the ID lists, and share the secondary partitioning layers with the default index. This effectively shares physical data structures across indexes and saves space. Figure 2a gives an example. The bottom offset lists are for a secondary vertex-bound index, which only consists of offset lists and no partitioning layers. Recall that since edge-bound indexes need to contain predicates between adjacent edges, this storage can only be used for vertex-bound indexes.
- *With predicates or different secondary partitioning*: In this case, the local views of the secondary index are different from the local views of the default index and we need to store new partitioning layers and an offset list layer, as shown in Figure 2b. This storage layout is used for edge-bound indexes as well as vertex-bound indexes that contain predicates.

We give the details of the memory page structures that store ID and offset lists in Section 4. In our evaluations, we demonstrate that for many applications, the memory footprint of secondary indexes can be very low, sometimes as low as a few percentage points.

We next address this question: *how much slower is reading ID lists through offset list indirections compared to sequential reads if the IDs were copied over (so requiring larger memory)?* We address this question in the context of an in-memory setting because our implementation is in an in-memory system. However, even in disk-based systems, lists are often brought to memory inside a single page and then read from memory during operations. So our offset list choice would primarily affect the speed of reading once an appropriate page is in memory. We performed the following demonstrative experiment. We took the popular and relatively large LiveJournal dataset, which contains 68M edges, and performed 5-hop enumeration queries from a random set of 100 source vertices. These queries form a stress test for our question because the main operation they perform is reading the IDs in adjacency lists and copying them over to tuples that are passed between operators. We kept the graph unlabelled, so added a single label to edges, and did not add any properties to the graph. We then evaluated the queries in three different ways:

(i) *Sequential:* Sequentially reading the system's default ID lists. This forms a baseline for the best cache locality we can obtain in our storage.

(ii) *List-level indirection:* Reading the system default ID lists through a vertex-bound index that sorts the edges in each list randomly. This achieves an indirection that is limited to within a list but we expect good CPU cache locality.

(iii) *Graph-level indirection:* To form a baseline for a very poor cache locality, we separately implement a new index that shuffles the adjacency lists into a single list and provides an indirection to each edge and neighbour ID pair. This effectively simulates an indirection where the random reads are not constrained to a list but can span 68M edges.

Sequential reads took 6.7s/query, reads through list-level indirections took 12.4s/query, and graph-level indirection took 63.3s/query. Therefore, even in this stress test, the list-level indirections were only 1.85x slower than reading directly form ID lists (and 5.1x faster than graph-level indirections). So despite reading through an indirection, we obtain a very good cache locality. As a reference to compare the memory consumption, implementing a secondary index that copies over IDs would double the storage in this experiment. Instead, the overhead of our vertex-bound index in this experiment is 1.13x. This is a very reasonable memory vs performance tradeoff, especially given that queries often perform other operations, e.g., read of edge and vertex properties, aggregations, or predicate evaluations, for which the performance slow down will be smaller, as those operations are not affected by this indirection.

# 4. IMPLEMENTATION DETAILS

## 4.1 Query Optimizer and Processor

A+ indexes are used in evaluating subgraph pattern component of queries, which is where the queries' joins are described. We give an overview of the relevant join operators and the optimizer of the system. Reference [32] describes the details of the EXTEND/INTERSECT operator and the dynamic programming join optimizer of the system in absence of the A+ indexes sub-system.

**JOIN OPERATORS:** EXTEND/INTERSECT (E/I) is the primary join operator of the system. Given a query $Q(V_Q, E_Q)$ and an input graph $G(V, E)$, let a *partial k-match* of $Q$ be a set of vertices of V assigned to the projection of $Q$ onto a set of $k$ query vertices. We denote a sub-query with $k$ query vertices as $Q_k$. E/I is configured to intersect $z{\geq}1$ adjacency lists that are sorted on neighbour IDs. The operator takes as input (k-1)-matches of $Q$, performs a $z$-way intersection, and extends them by a single query vertex to k-matches. For each (k-1)-match $t$, the operator intersect $z$ adjacency lists that are bound to the vertices of $t$ and extends $t$ with each vertex in the result of this intersection to produce $k$-matches. If $z$ is one, no intersection is performed, and the operator simply extends $t$ to each vertex in the adjacency list. The system uses E/I to generate plans that contain worst-case optimal join-style multi-way intersections.[2]

To generate plans that use A+ indexes, we extended E/I to take adjacency lists that can be bound to edges as well as vertices. We then added a variant of E/I that we call the **MULTI-EXTEND** operator, that performs intersections of adjacency lists that are sorted by properties other than neighbour IDs and extends partial matches to more than one query vertex. Specifically the operator is configured with $z{\geq}2$ adjacency lists to intersect and takes partial (k-z)-matches as input. For each (k-z)-match $t$, the operator intersect $z$ adjacency lists that are bound to either the edges or vertices of $t$ and produces $k$-matches. This allows us to have intersection-based query plans also for structurally acyclic queries.

**Dynamic Programming Optimizer:** GraphflowDB has a dynamic programming-based join optimizer. For each $k{=}1, ..., m{=}|V_Q|$, in order, the optimizer finds the lowest-cost plan for each sub-query $Q_k$ in two ways: (i) by considering extending every possible sub-query $Q_{k-1}$'s (lowest-cost) plan by an E/I operator; and (ii) if $Q$ has an equality predicate involving $z{\geq}2$ query edges, by considering extending smaller sub-queries $Q_{k-z}$ by a MULTI-EXTEND operator. At each step, the optimizer considers the edge and vertex labels and other predicates together, since secondary A+ indexes may be storing local views that contain predicates other than edge label equality. When considering possible $Q_{k-z}$ to $Q_k$ extensions, the optimizer queries the INDEX STORE to find both vertex- and edge-bound indexes that can be used that satisfies part or all of the predicates that would be involved in the extension. Then for each possible index combination retrieved, the optimizer enumerates a plan. After adding an E/I or MULTI-EXTEND operator, if there are any predicates that can be evaluated on $Q_k$ and not satisfied during the extension to $Q_k$ by the local views used, the optimizer adds a FILTER operator (effectively pushing down filters).

The systems' cost metric is *intersection cost* (i-cost), which is the total sizes of the adjacency lists that the system estimates will be accessed by the E/I and MULTI-EXTEND operators in a plan. The system uses a *subgraph catalogue* [32] that estimates the average lengths of different lists, e.g., forward list of each vertex or forward `Wire` list of each vertex. When estimating i-cost, if the adjacency lists that is used in an extension contains a predicate $p$ other than edge or vertex labels, we multiply the average length returned by the subgraph catalogue with the estimated selectivity of $p$.

[2]There is a second join operator HASHJOIN that takes sets of two partial matches $Q_{k1}$ and $Q_{k2}$ and hash-joins them on their common query vertices. HASHJOIN does not use A+ indexes, so is not relevant to our work in this paper.

## 4.2 Index Store

We implemented an INDEX STORE component that stores both the predicate and sorting criterion of each A+ index in the system. Every A+ index in the system, their type, secondary partitioning, sorting criteria, as well as additional predicates for secondary indexes are maintained in the INDEX STORE. The INDEX STORE is queried by the system's optimizer to find possible extensions of $Q_{k-z}$ sub-queries to $Q_k$. Specifically, the optimizer asks for the existence of possible vertex or edge-bound indexes, e.g., a vertex-bound index that satisfies edge label and `currency` equality predicates. The INDEX STORE inspects the predicates that are satisfied by the local views that correspond to each secondary partitioning level of each index and returns all indexes that can be used.

## 4.3 Physical Storage In Memory

Default and secondary vertex-bound A+ indexes are implemented using the same data structure that groups vertices into groups of 64 allocates one data page for each group. Vertex IDs are assigned consecutively starting from 0, so given an ID, with a division and mod operation we can access the first secondary partitioning level of a vertex. The nested secondary partitioning is implemented using a CSR-like format which points to either ID lists in the case of the default A+ indexes or offset lists in the case of secondary A+ indexes. The neighbour vertex and edge ID lists are stored as 4 byte integer and 8 byte long arrays. In contrast, the offset lists in both cases are stored as byte arrays by default. Offsets are variable-length, and we encode all offsets in an offset list with the maximum number of bytes needed for each offset. This encoding size is stored as a single byte header in the beginning of each offset list.

Edge-bound indexes are partitioned by edge IDs but access to the list of an edge requires not only the edge ID but also either the source or destination vertex ID of the edge that the offset lists will point to. For example, if $e7$'s offset list points to $v4$'s list, we need both $e7$ and $v4$ to access $e7$'s list. This vertex ID is always part of the intermediate tuple $t$ that will be extended and contains $e7$. Specifically, we store all the edges that point to the ID list of a vertex $v_i$ in a single page, which is accessed by $v_i$'s ID. All edge IDs in this page form the first partitioning layer on the page. The reason for this design is that, when updates arrive, and say $v4$'s ID list gets updated, we need to find all the possible edge ID lists that need to be updated, so we can directly use $v4$'s ID to access all these edge-bound lists.

## 4.4 Index Maintenance

Each vertex-bound data page, storing ID lists or offset lists, is accompanied with an update buffer. Each edge addition $e{=}(u, v)$ is first applied to the update buffers for $u$'s and $v$'s pages. Then we go over each vertex-bound A+ index $I$ in the INDEX STORE. If $I$'s global view contains a predicate $p$, we first apply $p$ to see if $e$ passes the predicate. If so, or if $I$ does not contain a predicate, we update the necessary update buffers for the offset list pages of $u$ and/or $v$. The update buffers' sizes are by default 20% of the sizes of their data page buffers and are merged into the actual data pages when the buffer is full. Edge deletions are handled by adding a "tombstone" for the location of the deletion until a merge is triggered.

Maintenance of an edge-bound A+ index `EB` is more involved. For an edge insertion $e{=}(u, v)$, we perform two separate operations. First, we check to see if $e$ should be inserted into the adja-

| Name | #Vertices | #Edges | Avg. degree |
|---|---|---|---|
| Orkut (Ork) | 3.0M | 117.1M | 39.03 |
| LiveJournal (LJ) | 4.8M | 68.5M | 14.27 |
| Wiki-topcats (WT) | 1.8M | 28.5M | 15.83 |
| BerkStan (Brk) | 685K | 7.6M | 11.09 |

Table 2: Datasets used.

cency list of any adjacent edge $e_b$ by running the predicate $p$ of EB on $e$ and $e_b$. For example, if EB is defined as Destination-Forward, we loop through all the backward adjacent edges of $u$ using the system's default vertex-bound index. This is equivalent to running two *delta-queries* as described in references [6, 25] for a continuous 2-path query. Second, we create a new list for $e$ and loop through another set of adjacency lists (in our example $v$'s forward adjacency list in D) and insert edges into $e$'s list.

# 5. EVALUATION

The goal of our experiments is two-fold. First, we demonstrate the flexibility and efficiency of our indexing sub-system on three very different popular applications that GDBMSs support: (i) labelled subgraph queries; (ii) recommendations; (iii) financial fraud detection. Existing adjacency list indexes of systems are not optimized to perform very fast joins on any of these applications. By either reconfiguring the system's default indexes or using new ones, we improve the performance of the system significantly, with low memory overheads. Second, we evaluate the performance and memory overhead tradeoffs offered by different A+ indexes on these workloads. We also present experiments benchmarking our index maintenance performance and baseline comparisons against Neo4j [33] and TigerGraph [46], which are two popular commercial GDBMSs.

## 5.1 Experimental Setup

We use a single machine that has two Intel E5-2670 @2.6GHz CPUs and 512 GB of RAM. The machine has 16 physical cores and 32 logical cores. For all experiments, we use a single physical core. We set the maximum JVM heap size to 500GB. Table 2 shows the datasets used. Our datasets include social, web, and Wikipedia knowledge graphs, which have a variety of graph topologies and sizes ranging from several million edges to over a hundred-million edges. A dataset G, denoted as $G_{i,j}$, has $i$ and $j$ randomly generated vertex and edge labels, respectively. We omit $i$ and $j$ when they are set to 1. We use query workloads drawn from real-world applications: (i) edge- and vertex-labelled subgraph queries; (ii) the MagicRecs recommendation engine from Twitter [19]; and (iii) fraud detection in financial transaction networks. The details of these applications and queries are explained in subsequent sections.

## 5.2 Default A+ Index Reconfiguration

We first demonstrate the benefit and overhead tradeoff of reconfiguring default A+ indexes in two different ways: (i) by only changing the sorting criteria; and (ii) by adding a new secondary partitioning. We used a popular subgraph query workload in graph processing that consists of labelled subgraph queries. In all systems work we are aware of, this workload consists of one of two variants: (a) queries with only edge labels [26, 32]; or (b) queries with only vertex labels [3, 9, 17, 22, 30, 45]. We take a natural and common third variant where both edges and vertices have labels.

We followed the data and subgraph query generation methodology from several prior work [10, 22, 32]. We took the 14 queries from reference [32] (omitted due to space reasons), which contain acyclic and cyclic queries with dense and sparse connectivity with up to 7 vertices and 21 edges. For each query we fixed the vertex and edge labels. We picked the number of labels for each dataset to ensure that queries would take time in the order of seconds to several minutes. Then we ran GraphflowDB on our workload on each of our datasets under three index configurations:

(i) D: system's default configuration, where edges are partitioned by edge labels and sorted by neighbour IDs.

(ii) $D_s$: keeps D's secondary partitioning but sorts edges first by neighbour vertex labels and then on neighbour IDs.

(iii) $D_p$: keeps D's sorting criteria and edge label partitioning but adds a new secondary partitioning on neighbour vertex labels.

Table 3 shows our results.[3] First observe that $D_s$ outperforms D on all of the 52 settings and by up to 10.38x and without any memory overheads as $D_s$ simply changes the sorting criteria of the indexes. Next observe that by adding an additional partitioning level on D, the joins get even faster consistently across all queries, e.g., $SQ_{13}$ improves from 2.36x to 3.84x on $Ork_{8,2}$, as the system can directly access edges with a particular edge label and neighbour label using $D_p$. In contrast, under $D_s$, the system performs binary searches inside lists to access the same set of edges. Even though $D_p$ is a reconfiguration, so does not index new edges, it still has minor memory overheads ranging from 1.05x to 1.15x because of the cost of storing the new partitioning layer. This demonstrates the flexibility A+ indexes gives to users to optimize the system to perform much faster on a different workload without any data remodelling, and with no or little memory overheads. Note that the consistent performance improvements we gain through reconfiguration also demonstrates that index reconfiguration does not hinder the quality of the plans our optimizer generates.

## 5.3 Secondary Vertex-Bound A+ Indexes

We next study the tradeoffs offered by secondary vertex-bound indexes. We use two sets of workloads drawn from real-world applications that benefit from using both the system's default A+ indexes as well as a secondary vertex-bound A+ index. Our two applications highlight two separate benefits users get from vertex-bound A+ indexes: (i) decreasing the amount of predicate evaluation; and (ii) allowing the system to generate new WCO-style join plans that are not possible with the default indexes only.

### 5.3.1 Avoiding Predicate Evaluation

In this experiment, we take a set of the queries drawn from the MagicRecs workload described in reference [19]. MagicRecs is a recommendation engine that was developed at Twitter that looks for the following patterns: for a given user $a_1$, it searches for users $a_2 ... a_k$ that $a_1$ has started following recently, and finds their common followers. These common followers are then recommended to $a_1$. We set $k$=2,3 and 4 in our workload. Our specific queries, $MR_1 ... MR_3$, are shown in Figure 3. These queries have a time predicate on the edges starting from $a_1$ which can benefit from indexes that sort on time. The second and third queries are also structurally cyclic, so can benefit from sorting on neighbour IDs, which is the default sorting order of our default A+ indexes. We evaluate our queries on all of our data sets on two index configurations. First is the system's default A+ indexes D as before. Second is:

(i) D+$VB_t$: adds a new secondary vertex-bound index $VB_t$ in the forward direction that: (i) has the same secondary partitioning as default forward A+ indexes, so shares the same partitioning layers as the default index; and (ii) sorts the most granular sublists on the `time` property of edges.

[3] Q14 is omitted as the query contained very few output tuples.

| | | $SQ_1$ | $SQ_2$ | $SQ_3$ | $SQ_4$ | $SQ_5$ | $SQ_6$ | $SQ_7$ | $SQ_8$ | $SQ_9$ | $SQ_{10}$ | $SQ_{11}$ | $SQ_{12}$ | $SQ_{13}$ | Mm |
|---|---|---|---|---|---|---|---|---|---|---|---|---|---|---|---|
| $Ork_{8,2}$ | D | 1.68 | 5.47 | 3.66 | 1.30 | 1.58 | 1.45 | 1.73 | 2.49 | 0.95 | 17.74 | 7536.9 | 54.86 | 131.5 | 2778 |
| | $D_s$ | 0.91 | 3.12 | 2.04 | 1.19 | 1.05 | 1.22 | 1.33 | 1.51 | 0.77 | 4.89 | 725.9 | 41.92 | 55.62 | 2778 |
| | | **(1.85x)** | **(1.75x)** | **(1.79x)** | **(1.09x)** | **(1.50x)** | **(1.19x)** | **(1.30x)** | **(1.65x)** | **(1.23x)** | **(3.63x)** | **(10.38x)** | **(1.31x)** | **(2.36x)** | **(1.0x)** |
| | $D_p$ | 0.68 | 2.61 | 1.35 | 0.97 | 0.77 | 0.60 | 1.30 | 1.46 | 0.60 | 3.89 | 704.9 | 28.32 | 34.22 | 3106 |
| | | **(2.48x)** | **(2.10x)** | **(2.71x)** | **(1.34x)** | **(2.05x)** | **(2.44x)** | **(1.33x)** | **(1.71x)** | **(1.25x)** | **(4.56x)** | **(10.69x)** | **(1.94x)** | **(3.84x)** | **(1.12x)** |
| $LJ_{2,4}$ | D | 1.47 | 7.87 | 6.46 | 1.69 | 1.59 | 1.60 | 1.91 | 3.35 | 4.07 | 41.54 | 807.8 | 397.1 | 468.8 | 1016 |
| | $D_s$ | 1.45 | 6.22 | 5.42 | 1.49 | 1.51 | 1.52 | 1.40 | 2.39 | 2.82 | 28.07 | 241.2 | 268.6 | 259.2 | 1016 |
| | | **(1.01x)** | **(1.27x)** | **(1.19x)** | **(1.13x)** | **(1.05x)** | **(1.05x)** | **(1.36x)** | **(1.40x)** | **(1.44x)** | **(1.48x)** | **(3.35x)** | **(1.48x)** | **(1.81x)** | **(1.0x)** |
| | $D_p$ | 1.04 | 5.18 | 4.64 | 1.09 | 0.98 | 1.08 | 1.07 | 1.85 | 2.26 | 25.86 | 235.63 | 235.85 | 161.82 | 1164 |
| | | **(1.41x)** | **(1.52x)** | **(1.39x)** | **(1.55x)** | **(1.62x)** | **(1.48x)** | **(1.79x)** | **(1.81x)** | **(1.80x)** | **(1.61x)** | **(3.43x)** | **(1.68x)** | **(2.90x)** | **(1.15x)** |
| $WT_{4,2}$ | D | 0.61 | 4.59 | 5.48 | 0.84 | 1.17 | 0.90 | 0.73 | 11.25 | 2.85 | 1116.2 | 340.0 | 487.8 | 767.5 | 713 |
| | $D_s$ | 0.37 | 2.43 | 3.50 | 0.69 | 0.71 | 0.65 | 0.61 | 3.93 | 1.36 | 697.9 | 77.11 | 319.0 | 386.8 | 713 |
| | | **(1.65x)** | **(1.89x)** | **(1.56x)** | **(1.22x)** | **(1.65x)** | **(1.38x)** | **(1.20x)** | **(2.87x)** | **(2.09x)** | **(1.60x)** | **(4.41x)** | **(1.53x)** | **(1.98x)** | **(1.0x)** |
| | $D_p$ | 0.32 | 2.09 | 3.05 | 0.55 | 0.59 | 0.54 | 0.61 | 2.86 | 1.09 | 639.7 | 76.32 | 259.1 | 235.7 | 795 |
| | | **(1.91x)** | **(2.20x)** | **(1.80x)** | **(1.53x)** | **(1.99x)** | **(1.66x)** | **(1.21x)** | **(3.94x)** | **(2.62x)** | **(1.74x)** | **(4.45x)** | **(1.88x)** | **(3.26x)** | **(1.12x)** |
| $Brk_{2,2}$ | D | 0.46 | 2.41 | 1.19 | 1.32 | 2.10 | 1.52 | 4.74 | 27.15 | 142.8 | 701.6 | 23.90 | 889.0 | 754.6 | 196 |
| | $D_s$ | 0.46 | 1.46 | 0.79 | 0.96 | 1.50 | 1.09 | 2.93 | 13.50 | 70.80 | 347.9 | 10.58 | 386.2 | 248.4 | 196 |
| | | **(1.00x)** | **(1.65x)** | **(1.51x)** | **(1.38x)** | **(1.40x)** | **(1.39x)** | **(1.62x)** | **(2.01x)** | **(2.02x)** | **(2.02x)** | **(2.26x)** | **(2.30x)** | **(3.04x)** | **(1.0x)** |
| | $D_p$ | 0.19 | 1.40 | 0.66 | 0.78 | 1.51 | 0.96 | 2.86 | 12.40 | 68.74 | 335.6 | 10.45 | 381.2 | 215.9 | 206 |
| | | **(2.42x)** | **(1.72x)** | **(1.80x)** | **(1.69x)** | **(1.39x)** | **(1.58x)** | **(1.66x)** | **(2.19x)** | **(2.08x)** | **(2.09x)** | **(2.29x)** | **(2.33x)** | **(3.49x)** | **(1.05x)** |

Table 3: Runtime (in seconds) and memory usage in MBs (Mm) evaluating subgraph queries using three different index configurations: D, $D_s$, and $D_p$ introduced in Section 5.2.

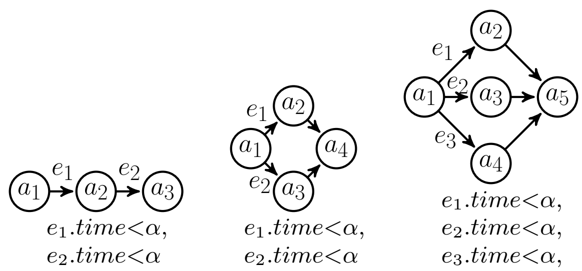


(a) $MR_1$. (b) $MR_2$. (c) $MR_3$.

Figure 3: MagicRec (MR) workload queries.

In our queries we set the value of $\alpha$ in the time predicate to have a 5% selectivity. For $MR_3$, on datasets LJ and Ork, we consider the query vertex $a_1$ fixed to 10000 and 7000 vertices, respectively for the queries to run within a reasonable time. Table 4 shows our results. First observe that despite indexing all of the edges again, our secondary index has only 1.08x memory overhead because of storing lightweight offset lists and sharing the partitioning layers. Creating a separate index would have given overheads closer to 50% (recall $VB_t$ is only a forward index). In return, we see up to 11.3x performance benefits. We note that our system uses exactly the same plans under both index configurations that start reading $a_1$, extends to its neighbours and finally performs a multiway intersection (except for $MR_1$, which is followed by a simple extension). The only difference is that under $D+VB_t$ the first set of extensions require fewer predicate evaluation because of accessing $a_1$'s adjacency list in $VB_t$, which is sorted on time. Overall this memory performance tradeoff demonstrates that with minimal overheads of an additional index, users obtain significant performance benefits on applications like MagicRecs that require fast response time.

| | | $MR_1$ | $MR_2$ | $MR_3$ | Mm |
|---|---|---|---|---|---|
| Ork | D | 29.37 | 255.4 | 22.65 | 2755 |
| | $D+VB_t$ | 14.36 | 166.3 | 3.33 | 2982 |
| | | **(2.05x)** | **(1.54x)** | **(6.80x)** | **(1.08x)** |
| LJ | D | 18.19 | 38.17 | 842.8 | 1689 |
| | $D+VB_t$ | 8.83 | 27.26 | 79.72 | 1820 |
| | | **(2.06x)** | **(1.40x)** | **(10.6x)** | **(1.08x)** |
| WT | D | 6.87 | 9.67 | 136.5 | 700 |
| | $D+VB_t$ | 2.69 | 5.36 | 22.74 | 755 |
| | | **(2.55x)** | **(1.80x)** | **(6.00x)** | **(1.08x)** |
| Brk | D | 1.15 | 1.73 | 7.53 | 191 |
| | $D+VB_t$ | 0.29 | 0.73 | 3.53 | 205 |
| | | **(3.97x)** | **(2.37x)** | **(2.13x)** | **(1.07x)** |

Table 4: Runtime (in seconds) and memory usage in MBs (Mm) evaluating the MagicRec queries using index configurations: D and $D+VB_t$ introduced in Section 5.3.1.

### *5.3.2 WCO Query Plans*

We next evaluate the benefit and overhead tradeoff of secondary vertex-bound indexes on an application where a secondary vertex-bound index can allow the system to generate new WCO join-style query plans that are not in the plan space of the system with default indexes. We take a set of queries drawn from cyclic fraudulent money flows that have been reported in prior literature [40], as well as acyclic patterns that contain the money flow paths from our running examples. Figure 4 shows our queries $MF_1$,...,$MF_5$. As an example, $MF_1$ searches for a cyclical flow that start and end in the same chequing accounts where two of the accounts in the path are in the same city. We will focus on $MF_1$ to $MF_4$ for now and use $MF_5$ in the next section. These four queries have equality conditions on the `city` property of the vertices, so can benefit from multiway intersections on `city`. We evaluate these queries on two index configurations. First is the system's default A+ indexes D as before. Second is:

(i) $D+VB_c$: which adds a new secondary vertex-bound index $VB_c$ in both forward and backward directions that: (i) has the same secondary partitioning as default A+ indexes; and (ii) sorts the most granular lists on neighbour's `city` property.

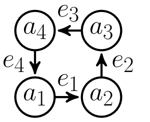

$a_i.acc{=}CQ$,
$a_2.city{=}a_4.city$

(a) $\mathrm{MF}_1$.

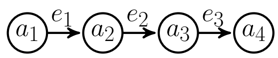

$a_1.city{=}a_2.city$,
$a_2.city{=}a_3.city$,
$a_3.city{=}a_4.city$

(b) $\mathrm{MF}_2$.

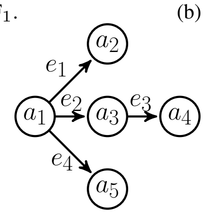

$a_2.city{=}a_4.city,\ \ a_4.city{=}a_5.city,$
$a_3.ID{<}10000,\ \ a_i.acc{=}CQ,\ \ a_5.acc{=}SV,$
$e_2.date{<}e_3.date,\ \ e_2.amt{>}e_3.amt,\ \ e_2.amt{<}e_3.amt{+}\alpha$

(c) $\mathrm{MF}_3$.

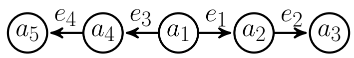

$a_1.city{=}\beta,\ \ a_2.city{=}a_4.city,$
$a_2.acc{=}CQ,\ \ a_3.acc{=}CQ,\ \ a_4.acc{=}SV,\ \ a_5.acc{=}SV,$
$e_1.date{<}e_2.date,\ \ e_1.amt{>}e_2.amt,\ \ e_1.amt{<}e_2.amt{+}\alpha$
$e_3.date{<}e_4.date,\ \ e_3.amt{>}e_4.amt,\ \ e_3.amt{<}e_4.amt{+}\alpha$

(d) $\mathrm{MF}_4$.

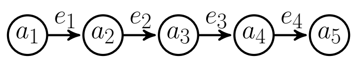

$a_1.ID{<}50000,\ \ a_i.acc{=}CQ,$
$e_1.date{<}e_2.date,\ \ e_1.amt{>}e_2.amt,\ \ e_1.amt{<}e_2.amt{+}\alpha,$
$e_2.date{<}e_3.date,\ \ e_2.amt{>}e_3.amt,\ \ e_2.amt{<}e_3.amt{+}\alpha,$
$e_3.date{<}e_4.date,\ \ e_3.amt{>}e_4.amt,\ \ e_4.amt{<}e_4.amt{+}\alpha$

(e) $\mathrm{MF}_5$.

Figure 4: Fraud detection workload queries.

We used LJ, WT, and Ork datasets[4] and randomly added each vertex an account type property from [CQ, SV], a city from 4417 cities, and to each edge an amount in the range of [1, 1000] and a date within a 5 year range. Table 5 shows our results (ignore the $\mathrm{MF}_5$ column and the D+VB$_c$+EB$_c$ rows for now). Similar to our previous experiment, despite indexing all of the edges (this time twice), our secondary index has only 1.17x memory overhead, whereas we see uniform improvements that are up to 24.7x. We note that in all of these queries, the benefits are solely coming from using new plans that use wco-style join processing. For example in query $\mathrm{MF}_1$, the D+VB$_c$ configuration allows the system to generate a plan that: (1) reads $a_1$; (2) uses MULTI-EXTEND to intersect $a_1$'s forward and backward lists in VB$_c$, which matches $a_2$ and $a_4$; and (3) uses E/I that intersects $a_2$'s forward and $a_4$'s backward lists in the default A+ index to match the $a_3$'s. Such plans are not possible in absence of the VB$_c$ index. Instead for $\mathrm{MF}_1$, under the default configuration, the system extends $a_1$ to $a_2$, then to $a_3$ separately, runs a FILTER operator to match the cities, and then uses E/I to match the $a_3$'s.

## 5.4 Secondary Edge-Bound A+ Indexes

Finally, we evaluate the tradeoffs that our secondary edge-bound A+ indexes on our financial fraud application from the previous section. We add a third configuration to our experiment:

[4] Brk is ignored as query run times are too small.

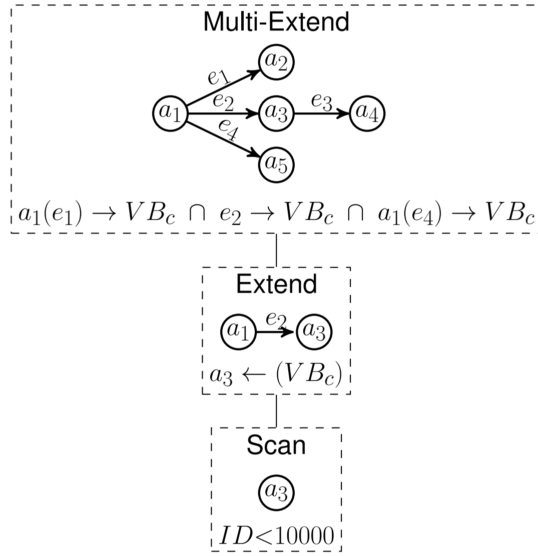


Figure 5: Plan for $\mathrm{MF}_3$ from Figure 4c with WCO join-style intersection using two VB$_c$ indexes and one EB$_c$ index introduced in Sections 5.3.2 and 5.4.

(i) D+VB$_c$+EB$_c$: adds the edge-bound index from Example 8 in Section 2.2.2. We change to grouping to be on v.$_{adj}$.acc instead of edge labels and add the predicate e.$_b$.amt < e.$_{nbr}$.amt + $\alpha$

We set the $\alpha$ "intermediate cut" value in our examples to have 5% selectivity. Table 5 shows our results. First we observe that the addition of EB$_c$ only allows new plans to be generated for $\mathrm{MF}_3$, $\mathrm{MF}_4$ and $\mathrm{MF}_5$, so we report numbers only for these queries. We see improvements ranging from 8.99x to up to 72.2x improvements for a 2.22x memory overheads. The performance improvements are primarily due to producing significantly more efficient plans that use the 2-path views in EB$_c$ index. For example, the system can now generate a new query plan for $\mathrm{MF}_3$. The plan is shown in Figure 5. The plan evaluates the query as follows: (1) scan $a_3$ nodes; (2) backward extend to match $a_1$'s; (3) use MULTI-EXTEND to perform an intersection, using $a_1$'s list in VB$_c$ twice and $e_2$'s list in EB$_c$. This is a highly complex plan that uses a mix of vertex- and edge-bound indexes and performs a 3-way intersections on a custom vertex property, which is automatically generated by our system. Such plans are not in the plan spaces of any system we are aware of.

The improvement and tradeoffs we report are examples and demonstrative in nature. The actual benefits and overheads of our indexes will naturally vary across workloads. For example, we have set the selectivity of the $\alpha$ parameter in the money flow patterns to 5% in our evaluations. This selectivity can have a significant impact on the actual benefits and overhead of edge-bound indexes. To demonstrate this we took the simplest money flow query that just searches for a single step flow from a vertex and varied $\alpha$ to be between a very small selectivity of 0.05% to a very high selectivity of 25% and built an accompanying edge-bound index. For each selectivity, we benchmarked using the edge bound to evaluate the query the edge bound index satisfies and compare with the performance of plans that used the system's default index. Table 6 shows our results. As expected, the lower the selectivity: (1) the more the performance benefits; and (2) the lower the memory footprint. For example, when selectivity is 0.05%, the benefits are as high as 35.6x while the memory overheads are only 1.28x. At a very high 25% selectivity, the benefits decrease to 16.7x while the overheads increase to 3.45x (albeit indexing 12.5x more edges than stored in the default A+ indexes).

| | | Q1 | Q2 | Q3 | Q4 | Q5 | Mem (MB) | $\lvert E_{indexed} \rvert$ |
|---|---|---|---|---|---|---|---|---|
| Ork | D | 73.35 | 5.53 | 32.85 | 71.46 | 890.8 | 2730 | 117.1 M |
| | D+VB$_c$ | 8.99 **(8.16x)** | 2.75 **(2.01x)** | 1.33 **(24.7x)** | 19.03 **(3.76x)** | — | 3183 **(1.17x)** | 117.1 M |
| | D+VB$_c$+EB$_c$ | — | — | 0.56 **(58.7x)** | 0.99 **(72.2x)** | 60.59 **(14.7x)** | 6000 **(2.20x)** | 513.2 M |
| LJ | D | 47.09 | 4.24 | 84.78 | 7.60 | 52.04 | 1649 | 68.5 M |
| | D+VB$_c$ | 11.45 **(4.11x)** | 2.86 **(1.48x)** | 5.12 **(16.6x)** | 3.66 **(2.08x)** | — | 1910 **(1.16x)** | 68.5 M |
| | D+VB$_c$+EB$_c$ | — | — | 2.16 **(39.3x)** | 0.39 **(19.5x)** | 5.79 **(8.99x)** | 3585 **(2.17x)** | 276.2 M |
| WT | D | 20.27 | 1.47 | 9.02 | 0.86 | 9.02 | 685 | 28.5 M |
| | D+VB$_c$ | 2.29 **(8.85x)** | 1.12 **(1.31x)** | 1.55 **(5.82x)** | 0.53 **(1.62x)** | — | 796 **(1.16x)** | 28.5 M |
| | D+VB$_c$+EB$_c$ | — | — | 0.50 **(18.0x)** | 0.14 **(6.14x)** | 0.79 **(11.4x)** | 1521 **(2.22x)** | 125.4 M |

Table 5: Runtime (in seconds) of Graphflow plans and memory usage (Mem) in MB evaluating fraud detection queries using different index configurations: D, D+VB$_c$, and D+VB$_c$+EB$_c$ introduced in Section 5.3.2. The run time speedups and memory size shown in parenthesis are in comparison to D.

| selectivity | 25% | 5% | 0.05% |
|---|---|---|---|
| D | 1028.8 | 1047.5 | 1056.3 |
| D+EB$_c$ | 61.66 **(16.7x)** | 47.77 **(21.9x)** | 29.71 **(35.6x)** |
| Mm(D+EB$_c$) | 5558 **(3.45x)** | 3116 **(1.93x)** | 1951 **(1.21x)** |
| $\lvert E_{indexed} \rvert$ | 1.466 B | 276.2 M | 2.9 M |

Table 6: Runtime (in secs) of for a 2-edge MoneyFlow path query on LJ using index configurations D and D+EB$_c$ introduced in Section 5.4. We report the number of indexed edges and memory (Mm) of D+EB$_c$ and compare it to D of size 1612 MB.

| | | SQ$_1$ | SQ$_2$ | SQ$_3$ | SQ$_{13}$ |
|---|---|---|---|---|---|
| LJ$_{12,2}$ | GF | 0.4 | 0.7 | 0.6 | 6.0 |
| | TG | 2.5**(6.3x)** | 11.8**(16.9x)** | 15.2**(25.3x)** | 30.5**(5.1x)** |
| | N4 | 29.3**(73.3x)** | 35.3**(50.4x)** | 36.8**(61.3x)** | $TL$ |
| WT$_{4,2}$ | GF | 0.5 | 2.1 | 3.1 | 235.7 |
| | TG | 1.6**(3.2x)** | 7.1**(3.4x)** | 10.2**(3.3x)** | 29.5**(0.1x)** |
| | N4 | 1.65k**(3300x)** | 876**(417.1x)** | 82.9**(26.7x)** | $TL$ |

Table 7: Graphflow (GF), TigerGraph (TG), and Neo4j (N4) run times in secs. Graphflow adjacency lists are grouped and sorted on edge and vertex labels, respectively. $TL$ indicates >30 mins.

## 5.5 Maintenance Performance

We next benchmark the maintenance speed of each type of A+ index on a micro-benchmark. We use two datasets LJ$_{2,4}$ and Brk$_{2,2}$. We load 50% of the dataset from the MagicRec application and insert the remaining 50% of the edges one at a time and evaluate the speed of 5 index configurations, each requiring progressively more maintenance work: (i) D$_s$ has no partitioning and a sort by the adjacent vertices IDs; (ii) D$_p$ partitions each adjacency list on adjacent edges `label`; (iii) D$_{ps}$ sorts each partition in D$_p$ by the adjacent vertices IDs; (iv) D$_{ps}$+VB$_t$ creates a secondary adjacency list index on time for D$_{ps}$; and finally (v) D$_{ps}$+EB$_t$: an edge bound adjacency list index with the same grouping and sorting as VB$_t$ for the query $v_s{-}[e_b]{\leftarrow}v_d{-}[e_{adj}]{\rightarrow}v_{adj}$ with predicate e$_b$.time < e$_{adj}$.time + $\alpha$ that has a 1% selectivity.

We ran our benchmark on LJ$_{2,4}$ and Brk$_{2,2}$. Using a single thread, we were able to maintain the following update rates per second (reported respectively for LJ$_{2,4}$ and Brk$_{2,2}$): 1.203M and 2.108M for D$_s$, 1.024M and 1.892M for D$_p$, 1.081M and 1.832M for D$_{ps}$, 706K and 1.691M for D$_{ps}$+VB$_t$, and 41K and 110K for D$_{ps}$+EB$_t$. Our update rate gets slower with additional complexity but we are able to maintain insert rates of between 50-100k edges/s for our edge-bound index and between 706K-2.1M for our vertex-bound indexes, using a single thread.[5]

## 5.6 Neo4j & TigerGraph Comparisons

We finish our evaluation by presenting GraphflowDB's performance against two popular GDBMSs. These experiments do not demonstrate the benefits and overheads of A+ indexes and are presented for completeness of our work and interested readers. We ran four of our labelled subgraph queries SQ$_1$, SQ$_2$, SQ$_3$, and SQ$_{13}$ on LJ$_{12,2}$ and WT$_{4,2}$ on Neo4j and TigerGraph, using their default configurations and using the D$_p$ configuration from Section 5.2 for GraphflowDB. Table 7 shows our results. GraphflowDB was faster on all queries except Q13 on WT$_{4,2}$, where TigerGraph was faster. SQ$_{13}$ is a long 5-edge path query. We are unaware of any publication that describes TigerGraph but our email communication with TigerGraph developers indicates the system is highly optimized for long path queries.

# 6. RELATED WORK

We reviewed adjacency lists in existing GDBMSs in our introductory section. We first review the Kaskade [16] query optimization framework that also uses materialized graph views. Then, we review related work in three areas: (i) indexes in RDF systems, another important class of DBMSs that support a graph-structured data model; (ii) adjacency lists in graph analytics systems; and (iii) indexes for queries other than the subgraph queries with predicates that we consider in this work.

As we observed earlier, our use of A+ indexes during query processing can be thought of as a specific query processing using views. There is a rich literature on using views to answer queries. We do not review this literature here and refer the reader to reference [20] for a survey.

**Kaskade [16]** (KSK) is a graph query optimization framework that uses *materialized graph views* to speed up query evaluation. Specifically, KSK takes as input a query workload $\mathcal{Q}$ and an input graph $G$. Then, KSK enumerates possible *views* for $\mathcal{Q}$, which are other graphs $G'$ that contain a subset of the vertices in $G$ and other edges that can represent multi-hop connections in $G$. For example, if $G$ is a data provenance graph with job and file vertices, and consumes and produces relationships between jobs and files, a graph

[5]For interested readers, we note that our guiding design principle in GraphflowDB is to implement it as a read-optimized system that takes bulk data ingests, instead of fast streams of transactional writes. This is instructed by a recent user survey of GDBMSs [41], where we observed that GDBMSs are rarely the transactional stores in enterprises. Instead, they are systems that often ingest data from relational systems to develop read-heavy applications that require complex and fast join processing.

view $G'$ could store only the job vertices and their dependencies through files if some queries only need these 2-hop relationships. KSK is a framework that selects a set of views for a workload, materializes them in Neo4j, and then translates queries over $G$ to appropriate graphs (views) that are stored in Neo4j, which is the final system that answers queries. Therefore, the overall framework is limited by Neo4j's adjacency lists. There are significant differences between the views A+ indexes effectively provide access to and KSK's views. First, KSK's views are based on "constraints" that are mined from $G$'s schema based only on vertex/edge labels and not properties. For example, KSK can mine "job vertices connect to jobs in 2-hops but not to file vertices" constraints but not "accounts connect to accounts in 2-hops with later dates and lower amounts", which is the predicate in our edge bound index (let alone partitioning these 2-hops by edge IDs). Therefore, KSK cannot enumerate a useful view for our money flow queries. Second, KSK views do not support flexible groupings, predicates, or sorting, and are only vertex ID partitioned (because graphs in Neo4j are only vertex ID partitioned). Finally, the overall framework is limited by Neo4j's query processor, which does not support WCO-style plans.

**Indexes in RDF Systems:** RDF systems support the RDF data model, in which data is represented as a set of (subject, predicate, object) triples. Because each triple can be seen as a labeled edge between a subject and an object, RDF is a graph-structured model. Prior work has introduced numerous architectural approaches to develop RDF systems such as: (1) using an underlying existing RDBMS [1, 2, 8, 12]; (2) storing and then indexing one large triple table [35, 48]; and (3) developing a system based on a native-graph storage, such as an adjacency list [51]. A comprehensive review of the designs of these systems is beyond the scope of our paper and we refer the reader to reference [39] for a survey of these approaches. These systems have different designs to further index these tables or their adjacency lists. For example, RDF-3X [35] indexes an RDF dataset in multiple B+ tree indexes for the six possible sort orders. As another example, the gStore system encodes several vertices in fixed length bit strings that captures information about the neighborhoods of vertices. Then these new encodings are stored in an index called *VS*$^*$-tree to prune certain parts of the graph during query processing. Similar to the GDBMSs we reviewed, these work also define fixed indexes for RDF triples. A+ indexes instead gives users flexibility by providing a mechanism for deciding which edges to index in adjacency lists so that they can tailor a GDBMS to the requirements of their workloads.

**Indexes in Graph Analytics Systems:** There are numerous graph analytics systems [7, 13, 23, 31, 42] that are designed to do batch analytics, such as decomposing a graph into connected components. These systems use native graph storage formats, such as adjacency lists or sparse matrices. Work in this space generally focuses on optimizing the physical layout of the edges in memory. For systems storing the edges in adjacency list structures, a common technique is to store them in a compressed sparse row (CSR) format [11], which we used in implementing our secondary *partitioning* in A+ indexes. References [15, 42] study CSR-like partitioning techniques for large lists and reference [50], proposes segmenting a graph stored in a CSR-like format to achieve better cache locality. This line of work is complementary to our work. Within the scope of this paper, we did not study how to optimize the adjacency lists with which we implemented A+ indexes and alternative physical storage structures can be used to store the edges in our A+ indexes. Finally, for analytics in the distributed setting, there is numerous work on different ways of partitioning the adjacency lists to reduce communication between workers performing a graph analytics. We do not review this work here and refer the reader to reference [27] for an introductory overview.

**Indexes For Advanced Queries:** Prior work have introduced advanced indexes for several classes of queries that we do not consider in our work:

*Complex subgraph queries:* Many prior algorithmic work on evaluating subgraph queries [14, 28, 29] have proposed auxiliary indexes that index subgraphs more complex than edges, such as paths, stars, or cliques. This line of work effectively demonstrates that indexing such subgraphs can speed subgraph query evaluation. It is worth mentioning that A+ indexes can be generalized to index more complex subgraphs that are partitioned by vertices or edges. Within the scope of our work, we designed A+ indexes to bring enough flexibility to the applications we are aware of that use GDBMSs without this additional complexity.

Some other algorithmic work focus on evaluating highly complex subgraph queries, e.g., those that contain up to hundreds of vertices and edges. Some of these work, such as CFL [10], $\text{DP}_{\text{ISO}}$ [21], and $\text{Turbo}_{\text{ISO}}$ [22] develop query-specific auxiliary indexes. These indexes are often more complex than A+ indexes, and are tightly designed for a specific subgraph matching algorithm. Existing GDBMSs do not process queries with those algorithms and rely on traditional relational operators, such as joins, filters, and scans. Therefore it seems difficult to integrate these indexes into GDBMSs, without changing their query processors. Instead as we demonstrated, our A+ indexes are easy to integrate into existing GDBMSs. Whether or not one can decompose these complex queries into traditional DBMS operators to integrate these complex algorithms into GDBMSs is an interesting research direction.

*Indexes for Recursive Queries:* Several work also develop specialized indexes for recursive queries, such as shortest paths, reachability, and regular path queries (RPQ). We designed A+ indexes for (fixed) subgraph queries with arbitrary predicates, so the indexes proposed in this line of work is less related to our work, so we omit a detailed review of these indexes. As an example, using *landmark* vertices is a popular technique that has been used for shortest paths [5, 43], reachability [49], as well as RPQs [47]. Intuitively, these indexes store paths to a set of central vertices in the graph, and use these indexed paths during query processing.

# 7. CONCLUSION

Ted Codd, the inventor of the relational model, criticized the GDBMSs of the time as being restrictive because they only performed a set of "predefined joins" [44], which causes physical data dependence and contrasts with relational systems that can join arbitrary tables on arbitrary columns with the same data type. This is indeed still true to a good extent for contemporary GDBMSs, which are designed to join vertices with only their neighbourhoods, which are predefined to the system as edges and accessing these indexes when performing joins. However, this is specifically the major appeal of GDBMSs, as GDBMSs are highly optimized to perform these joins in a very fast manner, primarily by using adjacency list indexes to store input edges. Our work was motivated by the shortcoming that existing GDBMSs do not provide any flexibility in their adjacency list structures so a wider range of applications can benefit from their fast join capabilities. As a solution, we described a new indexing sub-system A+ indexes, that are coupled with a limited set of materialized views, which are conducive to a very lightweight implementation. We described our design and implementation of A+ indexes, demonstrated their flexibility, and evaluated the performance and memory tradeoffs they offer on a variety of applications drawn from popular real-world applications that use GDBMSs.

## 8. REFERENCES


[1] D. J. Abadi, A. Marcus, S. Madden, and K. Hollenbach. SW-Store: A Vertically Partitioned DBMS for Semantic Web Data Management. *The VLDB Journal*, 18(2), 2009.

[2] D. J. Abadi, A. Marcus, S. Madden, and K. J. Hollenbach. Scalable Semantic Web Data Management Using Vertical Partitioning. In *VLDB*, 2007.

[3] E. Abdelhamid, I. Abdelaziz, P. Kalnis, Z. Khayyat, and F. Jamour. Scalemine: Scalable Parallel Frequent Subgraph Mining in a Single Large Graph. In *SC*, 2016.

[4] C. R. Aberger, A. Lamb, S. Tu, A. Nötzli, K. Olukotun, and C. Ré. EmptyHeaded: A Relational Engine for Graph Processing. *TODS*, 42(4), 2017.

[5] T. Akiba, Y. Iwata, and Y. Yoshida. Fast Exact Shortest-Path Distance Queries on Large Networks by Pruned Landmark Labeling. In *ACM SIGMOD*, 2013.

[6] K. Ammar, F. McSherry, S. Salihoglu, and M. Joglekar. Distributed Evaluation of Subgraph Queries Using Worst-case Optimal and Low-Memory Dataflows. *PVLDB*, 11(6), 2018.

[7] Apache Giraph. https://giraph.apache.org.

[8] Apache Jena. https://jena.apache.org.

[9] B. Bhattarai, H. Liu, and H. H. Huang. CECI: Compact Embedding Cluster Index for Scalable Subgraph Matching. In *ACM SIGMOD*, 2019.

[10] F. Bi, L. Chang, X. Lin, L. Qin, and W. Zhang. Efficient Subgraph Matching by Postponing Cartesian Products. In *ACM SIGMOD*, 2016.

[11] A. Bonifati, G. H. L. Fletcher, H. Voigt, and N. Yakovets. *Querying Graphs*. Morgan & Claypool Publishers, 2018.

[12] M. A. Bornea, J. Dolby, A. Kementsietsidis, K. Srinivas, P. Dantressangle, O. Udrea, and B. Bhattacharjee. Building an Efficient RDF Store Over a Relational Database. In *ACM SIGMOD*, 2013.

[13] A. Buluç and J. R. Gilbert. The Combinatorial BLAS: Design, Implementation, and Applications. *International Journal of High Performance Computing Applications*, 25(4), 2011.

[14] J. Cheng, J. X. Yu, B. Ding, P. S. Yu, and H. Wang. Fast Graph Pattern Matching. In *ICDE*, 2008.

[15] F. Claude and G. Navarro. Extended Compact Web Graph Representations. In *Algorithms and Applications: Essays Dedicated to Esko Ukkonen on the Occasion of His 60th Birthday*. Springer-Verlag, 2010.

[16] J. M. F. da Trindade, K. Karanasos, C. Curino, S. Madden, and J. Shun. Kaskade: Graph views for efficient graph analytics. *CoRR*, abs/1906.05162, 2019.

[17] M. Elseidy, E. Abdelhamid, S. Skiadopoulos, and P. Kalnis. GRAMI: Frequent Subgraph and Pattern Mining in a Single Large Graph. *PVLDB*, 7(7), 2014.

[18] Gaussdb. https://e.huawei.com/en/solutions/cloud-computing/big-data/gaussdb-distributed-database.

[19] P. Gupta, V. Satuluri, A. Grewal, S. Gurumurthy, V. Zhabiuk, Q. Li, and J. Lin. Real-time Twitter Recommendation: Online Motif Detection in Large Dynamic Graphs. *PVLDB*, 7(13), 2014.

[20] A. Y. Halevy. Answering queries using views: A survey. *The VLDB Journal*, 2001.

[21] M. Han, H. Kim, G. Gu, K. Park, and W.-S. Han. Efficient Subgraph Matching: Harmonizing Dynamic Programming, Adaptive Matching Order, and Failing Set Together. In *ACM SIGMOD*, 2019.

[22] W.-S. Han, J. Lee, and J.-H. Lee. Turboiso: Towards Ultrafast and Robust Subgraph Isomorphism Search in Large Graph Databases. In *ACM SIGMOD*, 2013.

[23] S. Hong, H. Chafi, E. Sedlar, and K. Olukotun. Green-Marl: A DSL for Easy and Efficient Graph Analysis. In *ASPLOS*, 2012.

[24] Janus Graph. https://janusgraph.org.

[25] C. Kankanamge, S. Sahu, A. Mhedbhi, J. Chen, and S. Salihoglu. Graphflow: An Active Graph Database. In *ACM SIGMOD*, 2017.

[26] K. Kim, I. Seo, W.-S. Han, J.-H. Lee, S. Hong, H. Chafi, H. Shin, and G. Jeong. TurboFlux: A Fast Continuous Subgraph Matching System for Streaming Graph Data. In *ACM SIGMOD*, 2018.

[27] V. Kumar, A. Grama, A. Gupta, and G. Karypis. *Introduction to Parallel Computing: Design and Analysis of Algorithms*. Addison-Wesley, 1994.

[28] L. Lai, L. Qin, X. Lin, and L. Chang. Scalable Subgraph Enumeration in MapReduce. *PVLDB*, 8(10), 2015.

[29] L. Lai, L. Qin, X. Lin, Y. Zhang, L. Chang, and S. Yang. Scalable Distributed Subgraph Enumeration. *PVLDB*, 10(3), 2016.

[30] L. Lai, Z. Qing, Z. Yang, X. Jin, Z. Lai, R. Wang, K. Hao, X. Lin, L. Qin, W. Zhang, Y. Zhang, Z. Qian, and J. Zhou. Distributed Subgraph Matching on Timely Dataflow. *PVLDB*, 12(10), 2019.

[31] G. Malewicz, M. H. Austern, A. J. C. Bik, J. C. Dehnert, I. Horn, N. Leiser, and G. Czajkowski. Pregel: A System for Large-Scale Graph Processing. In *ACM SIGMOD*, 2010.

[32] A. Mhedhbi and S. Salihoglu. Optimizing Subgraph Queries by Combining Binary and Worst-Case Optimal Joins. *PVLDB*, 12(11), 2019.

[33] Neo4j. https://neo4j.com.

[34] Neo4j Property Graph Model. https://neo4j.com/developer/graph-database, 2019.

[35] T. Neumann and G. Weikum. RDF-3X: A RISC-style Engine for RDF. *PVLDB*, 1(1), 2008.

[36] H. Ngo, C. Ré, and A. Rudra. Skew Strikes Back: New Developments in the Theory of Join Algorithms. *SIGMOD Record*, 42(4), 2014.

[37] H. Q. Ngo, E. Porat, C. Ré, and A. Rudra. Worst-case Optimal Join Algorithms. In *PODS*, 2012.

[38] openCypher. https://www.opencypher.org.

[39] M. T. Özsu. A Survey of RDF Data Management Systems. *Frontiers of Computer Science*, 10(3), 2016.

[40] X. Qiu, W. Cen, Z. Qian, Y. Peng, Y. Zhang, X. Lin, and J. Zhou. Real-Time Constrained Cycle Detection in Large Dynamic Graphs. *PVLDB*, 11(12), 2018.

[41] S. Sahu, A. Mhedbhi, S. Salihoglu, J. Lin, and M. T. Özsu. The Ubiquity of Large Graphs and Surprising Challenges of Graph Processing: Extended Survey. *The VLDB Journal*, 2019.

[42] J. Shun, G. E. Blelloch, J. Shun, and G. E. Blelloch. Ligra: A Lightweight Graph Processing Framework for Shared Memory. *ACM SIGPLAN Notices*, 48(8), 2013.

[43] C. Sommer. Shortest-Path Queries in Static Networks. *ACM Computing Surveys*, 46(4), 2014.

[44] Edgar f. ("ted") codd turing award lecture. https://amturing.acm.org/award_winners/

codd_1000892.cfm.

[45] C. H. C. Teixeira, A. J. Fonseca, M. Serafini, G. Siganos, M. J. Zaki, and A. Aboulnaga. Arabesque: A System for Distributed Graph Mining. In *SOSP*, 2015.

[46] TigerGraph. https://www.tigergraph.com.

[47] L. D. J. Valstar, G. H. L. Fletcher, and Y. Yoshida. Landmark Indexing for Evaluation of Label-Constrained Reachability Queries. In *ACM SIGMOD*, 2017.

[48] C. Weiss, P. Karras, and A. Bernstein. Hexastore: Sextuple Indexing for Semantic Web Data Management. *PVLDB*, 1(1), 2008.

[49] Y. Yano, T. Akiba, Y. Iwata, and Y. Yoshida. Fast and Scalable Reachability Queries on Graphs by Pruned Labeling with Landmarks and Paths. In *CIKM*, 2013.

[50] Y. Zhang, V. Kiriansky, C. Mendis, S. Amarasinghe, and M. Zaharia. Making Caches Work for Graph Analytics. In *IEEE Big Data*, 2017.

[51] L. Zou, M. T. Özsu, L. Chen, X. Shen, R. Huang, and D. Zhao. gStore: A Graph-Based SPARQL Query Engine. *The VLDB Journal*, 23(4), 2014.